JOURNAL OF MECHANICS OF CONTINUA AND MATHEMATICAL SCIENCES
www.journalimcms.org

ISSN (Online) : 2454 -7190 Vol.-20, No.-3, March (2025) pp 24 - 35 ISSN (Print) 0973-8975

EXPERIMENTAL STUDY ON CRACK AND DEFORMATION IN REINFORCED CONCRETE BEAMS USING DIGITAL IMAGE CORRELATION

Didar Meiramov[1], Huynjin Ju[2], Hae-Chang Cho[3]

[1] Department of Architecture and Architectural Engineering, Hankyong National University, Jungang-ro 327, Anseong 17579, Gyeonggi Republic of Korea.

[2] School of Architecture and Architectural Engineering, Hankyong National University, Jungang-ro 327, Anseong 17579, Gyeonggi, Republic of Korea.

[3] Technology Center, Dream Structural Engineering Co. Ltd., Dongtan-daero 21-gil 10, Hwaseong 18471, Gyeonggi, Republic of Korea.

Email: [1] didar.sayatovich@gmail.com, [2]hju@hknu.ac.kr, [3]hc.cho@dreamse.co.kr

Corresponding Author: **Huynjin Ju**

https://doi.org/10.26782/jmcms.2025.03.00003

(Received: January 20, 2025; Revised: February 25, 2025; Accepted: March 8, 2025)

Abstract

The evaluation of cracking and displacement in reinforced concrete beams is critical for assessing structural performance and stiffness during service. The effectiveness of the digital image correlation (DIC) method was investigated for evaluating cracks and displacements in reinforced concrete beams. The beams had varying reinforcement ratios and concrete covers as key parameters. Specimens were tested under two-point loading, and the results were recorded using traditional measurement instruments. These results were then compared with the DIC results. The findings demonstrate that the DIC method accurately determines midspan deflection, with a minor error of 2.33% compared to traditional measuring instruments. However, the accuracy of crack width measurements varied due to elastic deformation, with errors ranging from 7.41% to 68% compared to those obtained by crack detectors. These results demonstrate the potential of the DIC method as a reliable tool for detailed analysis of cracking and deformation in reinforced concrete structures, though further refinement may be required for crack width assessment.

Keywords: Correlation, Cracking, Crack propagation, Digital image, Experiment, Reinforced concrete.

I. Introduction

Beams are fundamental structural elements in reinforced concrete (RC) structures, designed to withstand various sustained loads. These loads induce deflection, leading to the formation of cracks. Cracking occurs when the bending moment generates stresses that exceed the concrete's tensile strength, particularly at the bottom of the beam. In a simply supported beam under vertical loading, flexural cracks typically form near the mid-span, while shear cracks emerge near the supports to alleviate strain in the concrete. These cracks significantly impact the beam's performance, reducing stiffness, ductility, and serviceability, while also increasing the risk of reinforcement corrosion.

Numerous research has been conducted in the past to study the fracture mechanics of cracks [II], crack spacing [III], and crack propagation [VII, VIII, XIV] in RC members. In addition, numerous experiments have been conducted on different types of concrete, including lightly reinforced concrete [VI] or fiber-reinforced concrete [V, VII, and XIX], to analyze the cracking behavior.

The development of visual image scanning technologies that allow the monitoring of structures based on 3D or 2D scanning has opened new opportunities for researchers in various fields [XII]. With the emergence of the digital image correlation (DIC) method, which is a non-destructive technique based on the images on the surface of specimens to measure deformations [XIII], crack propagation in reinforced concrete members[XV]. Verbruggen et al. [XX], Sindu and Sasmal [XVII], Lacidogna et al. [XI], and Tambusay A. et al. [XIV] conducted flexural and direct tensile concrete tests using the DIC method. Aryanto et al. also used the DIC method to evaluate the deformation and crack propagation of plain, fiber and reinforced concrete and compared the DIC results with the conventional instrument readings. The DIC results matched well with the experimental measurements for crack development and crack patterns for all types of concrete [I]. Huang et al. studied the cracking of concrete under micro-scale DIC analysis taking the water-cement ratio as a key variable and found out that for the concrete with a high water-cement ratio, most cracks cross the interface transition zone and only a few cracks appear in the coarse aggregate [IX]. Seemab et al. developed a model for crack localization and propagation of shear cracks in RC beams without shear reinforcement using the DIC method [XVI, XVIII, XIX].

Previous studies using the DIC method often relied on single crack width data to validate the accuracy of the DIC analysis. However, conclusions based on single crack measurements can be misleading, as they do not provide a comprehensive view of the overall cracking behavior. To address this limitation, this study focuses on directly evaluating the total crack width from strain data using an integration method. This method ensures the accuracy of the DIC analysis by comparing its results with those from traditional measurement instruments used on reinforced concrete (RC) beams under two-point loading. Six RC beams were cast using normal-strength concrete, with variations in reinforcement ratio and concrete cover as key variables in the analysis. The findings of this study contribute to the advancement of using the DIC method for structural health monitoring of RC structures.

II. Materials and Methods

Specimen details

Six RC beams were cast and tested to analyze the load-deformation relationship and crack propagation. Table 1 and Figure 1 present the specimen details including the beam dimensions with reinforcement details. All the specimens had a total length of 4,900 mm. The reinforcement ratio and concrete cover were considered key variables. The specimens had two D-13 compressive longitudinal reinforcements and three tensile longitudinal reinforcements varying from D13, D16, and D19. The concrete cover distance from the bottom of the specimen to the surface of the stirrup was either 23.5 mm or 53.5 mm, as shown in Figure 1(a). In addition, D10 stirrups were placed at 155 mm spacing for shear reinforcement, except in the pure bending moment region, as shown in Figure 1(b). The material properties of the concrete at 28 days after pouring and of the reinforcing steels were tested and are presented in Table 2.

Table 1: Specimen details

No.	Specimen	Dimensions (mm)	Total length (mm)	Top rebars	Bottom rebars	Reinforcement ratio
1	A-13	350x250	4500	2-D13	3-D13	0.49%
2	A-16				3-D16	0.77%
3	A-19				3-D19	1.11%
4	B-13	380x250			3-D13	0.49%
5	B-16				3-D16	0.77%
6	B-19				3-D19	1.11%

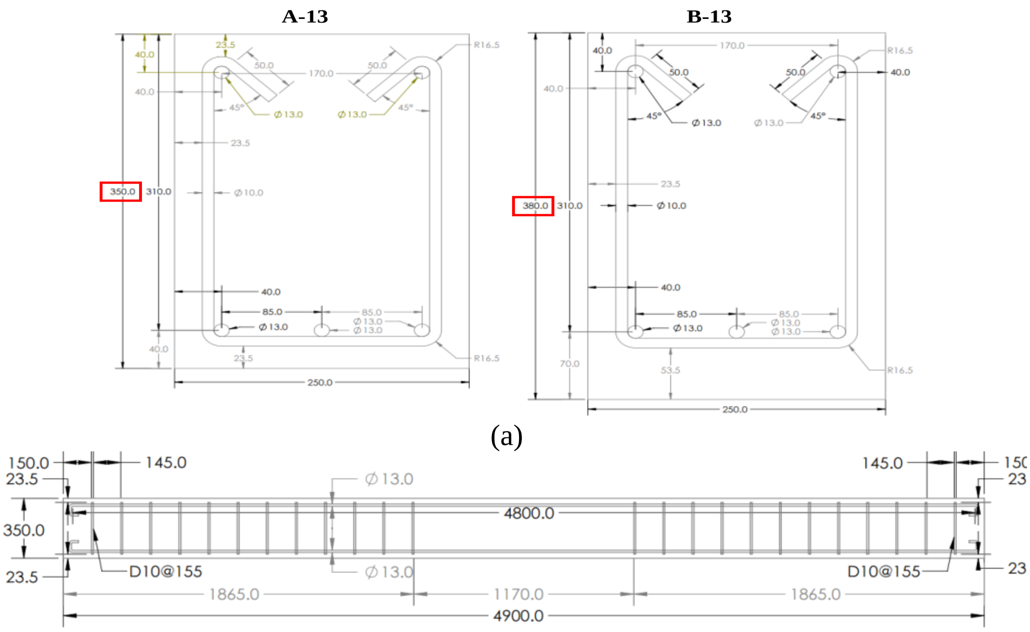

(b)

Fig. 1. Beam dimensions (in mm): (a) side view; (b) front view

Table 2: Measured material properties

Concrete			Longitudinal rebars			Transverse stirrups		
E	f_{ck}	f_r	E	f_y	f_u	E	f_y	f_u
25,811	28	2.3	200,000	531	668	200,000	471	542

DIC and Experimental setup

Figure 2 shows the load application and measuring instrumentation configuration for the specimens. All specimens were tested under two-point loading. The beams were simply supported at the locations 200 mm away from both ends, resulting in a 4,500 mm span length. A hydraulic actuator with a capacity of 1,000 kN was used to apply the load. The top of the specimen was subjected to two equal vertical loads with a 1,500 mm distance between the load points.

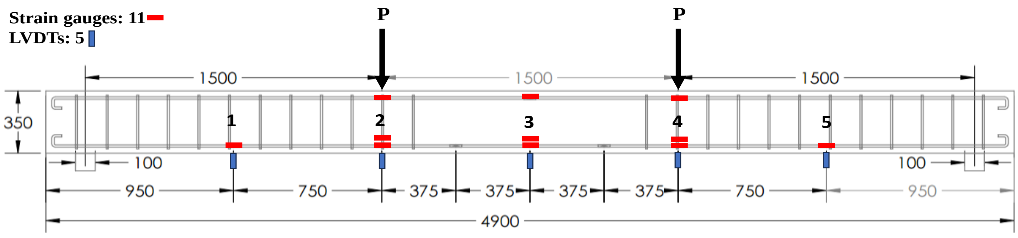

Fig. 2. Load application and measuring instrument configuration

Figure 2 shows the instrument configuration. 5 linear variable differential transformers (LVDT) were used to measure deflections and 11 strain gauges were installed to measure strains, respectively, in the specimens. A MegaSpeed X9 Pro camera with a sensor with a pixel size of 10 μm, a focal length of 50 mm, and a maximum image resolution was 1920 x 1080 pixels for taking the digital images under load as shown in Figure 3. The camera was at a certain fixed distance from the beam and on the level perpendicular to the beam surface. The target surface of the specimens was prepared with irregular speckles for the DIC tracking algorithm software to work correctly [X]. Light-emitting devices were used to illuminate two ends of the specimen at a fixed distance so that all reference points could be extracted by image processing. The deformation and displacement fields were obtained using the open-source 2D DIC Matlab software Ncorr [IV]. Since the shape of the black speckles was irregular, and in addition, Ncorr software uses sophisticated filtering algorithms to decrease the likelihood of errors.

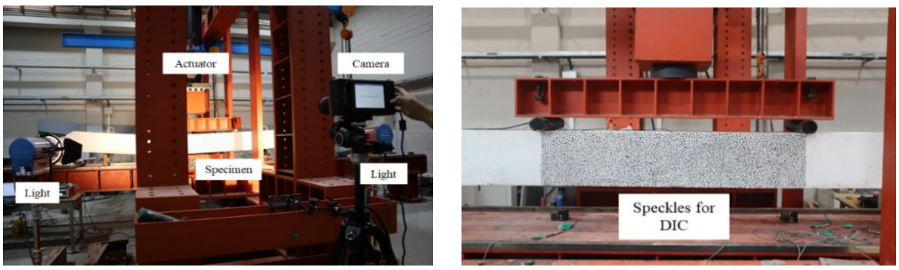

Fig. 3. DIC and loading test setup

Due to the relatively long span length of 4,500 mm, only the area between the two loading points, which is 1,500 mm, known as the theoretical bending moment zone, was recorded by the DIC method. This area was chosen because most cracks and maximum displacements occur in this region. The test was performed with displacement control at a rate of 0.5 mm/min, enabling clear monitoring of crack initiation and progression. DIC images were taken every 5 mm of displacement. In addition, the crack width was measured experimentally using a Langry LR-FK202 digital crack width detector at 4 load steps to compare the experimental crack width with the DIC results.

III. Results and Discussions

Load-deflection relationship

Figure 4 shows the load-displacement responses of the beams based on the measurements of LVDT and DIC. The red markers represent the displacement measurements obtained from the DIC analysis, while the black lines show the displacement measured by the LVDT at the midspan. Although six specimens were tested, specimen A13 has been excluded from the analysis because its supports were incorrectly installed. As shown in Figure 4, the deflection at yielding load increases according to the reinforcement ratio and concrete cover thickness. Overall, the DIC measurements at the midspan are quite fit for the LVDT measurements in all specimens in terms of vertical displacement.

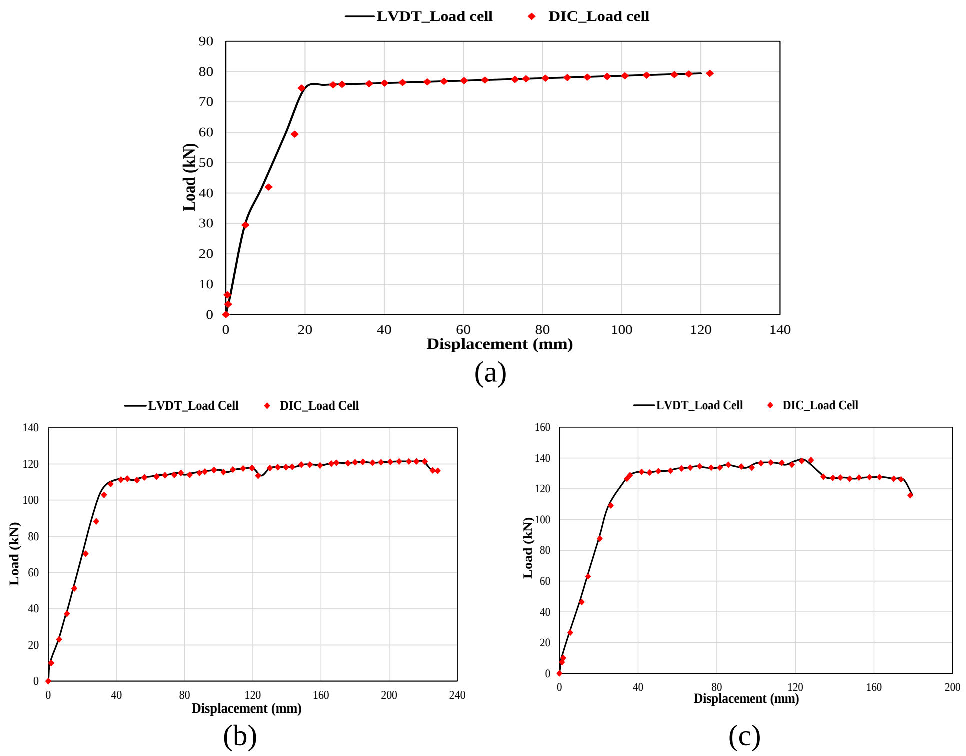

(a)

(b)

(c)

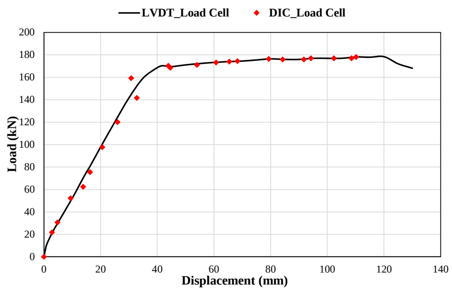

(d)

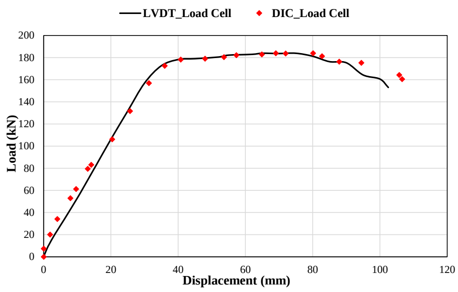

(e)

Fig. 4. Comparison of the load-displacement responses from LVDT and DIC measurements of the displacement at failure: (a) B13 (b) A16 (c) B16 (d) A19 (e) B19

Figure 5 shows the displacement contours of the beam at the failure obtained from the DIC analysis. The red color indicates that the deformation is significant, while darker shades of blue indicate minimal or close to zero deformation, as shown by the color scale. Figure 5 reveals that the DIC method well captured the asymmetrical displacement in the specimens such as B16 and B19 which experienced compressive crushing failure in the concrete section and it can be found as the sharp color transition in Figure 5. Consequently, the deflection in these areas is greater than on the other sides. For other specimens, the maximum displacement occurred at the midspan of the specimens.

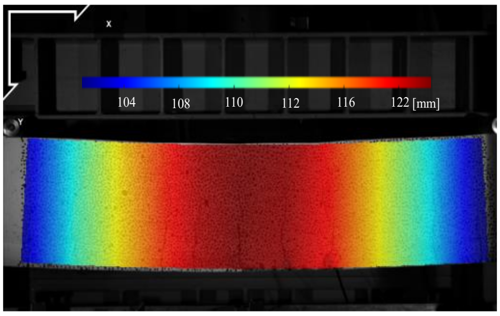

(a)

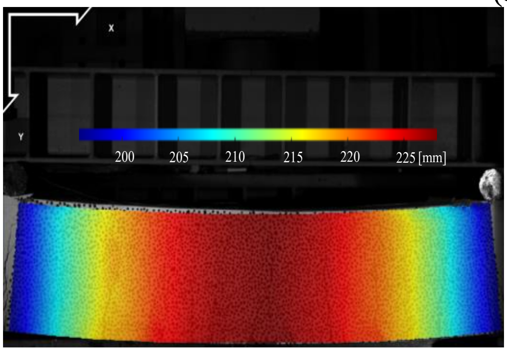

(b)

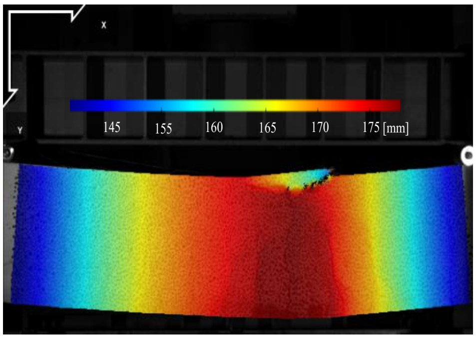

(c)

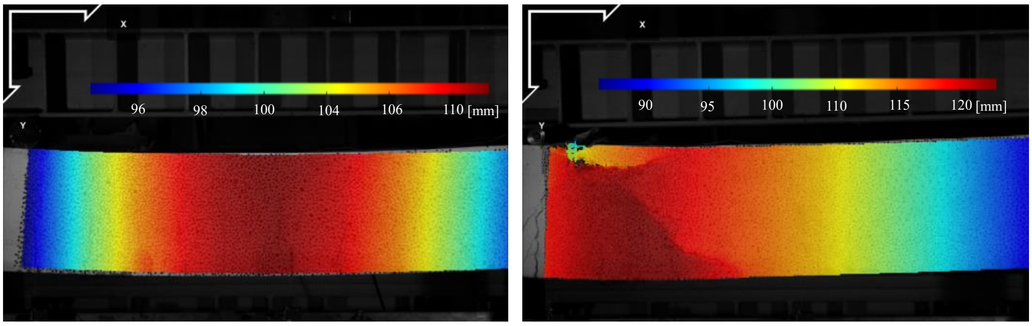

(d) (e)

Fig. 5. Vertical displacement contours of beams at the failure obtained from the DIC analysis: (a) B13 (b) A16 (c) B16 (d) A19 (e) B19

The peak loads and corresponding deflections obtained by LVDT and DIC for all beams are shown in Table 3. The results show that there is an increase in load capacity indicated by a higher peak load with increasing reinforcement ratios. In addition, the influence of the concrete cover is also found to be significant in the increase of load capacity. Based on the results, the DIC data showed an almost similar load-displacement trend, and the difference was within 2.33% as compared to the LVDT results, highlighting the effectiveness of the DIC method. The LVDT was placed at the bottom of the midspan to measure maximum displacement. At the high loading state, the specimen experienced large deformations causing the LVDT at the midspan of the beam distorted. It might result in a discrepancy between the measurements of the DIC and LVDT. In addition, such discrepancy may be attributed to the DIC algorithm and circumstances such as light and camera [20]. Despite such factors, it can be concluded that a maximum error of 2.33% is acceptable and it demonstrates the applicability of the DIC method.

Table 3 : Summary of the experimental load-displacement

Specimens	Maximum load	LVDT displacement	DIC displacement	Difference
B-13	79.42 kN	120 mm	122.24 mm	1.87%
A-16	121.40 kN	205 mm	205.84 mm	0.41%
B-16	138.57 kN	125 mm	127.91 mm	2.33%
A-19	178.12 kN	110 mm	110.18 mm	0.17%
B-19	183.94 kN	65 mm	64.87 mm	0.20%

Crack measurement

Figure 6 presents the strain contours of the beams at the failure state, as determined by the DIC analysis. These contours highlight the areas of local strain accumulation in the section of the specimens subjected to tension, which correspond to cracks. These regions of high strain are indicated in red. The DIC analysis effectively captured the crack propagation in the specimens. From the observation of the strain contours, it can be seen that specimens with thicker concrete cover exhibited a greater number of cracks but with lower strain accumulation intensity. In contrast, specimens with thinner concrete cover showed fewer cracks but with higher strain accumulation intensity. A similar trend was found with the reinforcement ratio; specimens with a higher reinforcement ratio displayed an increased number of cracks. These findings emphasize the impact of concrete cover thickness and reinforcement ratio on the cracking behavior of RC structures.

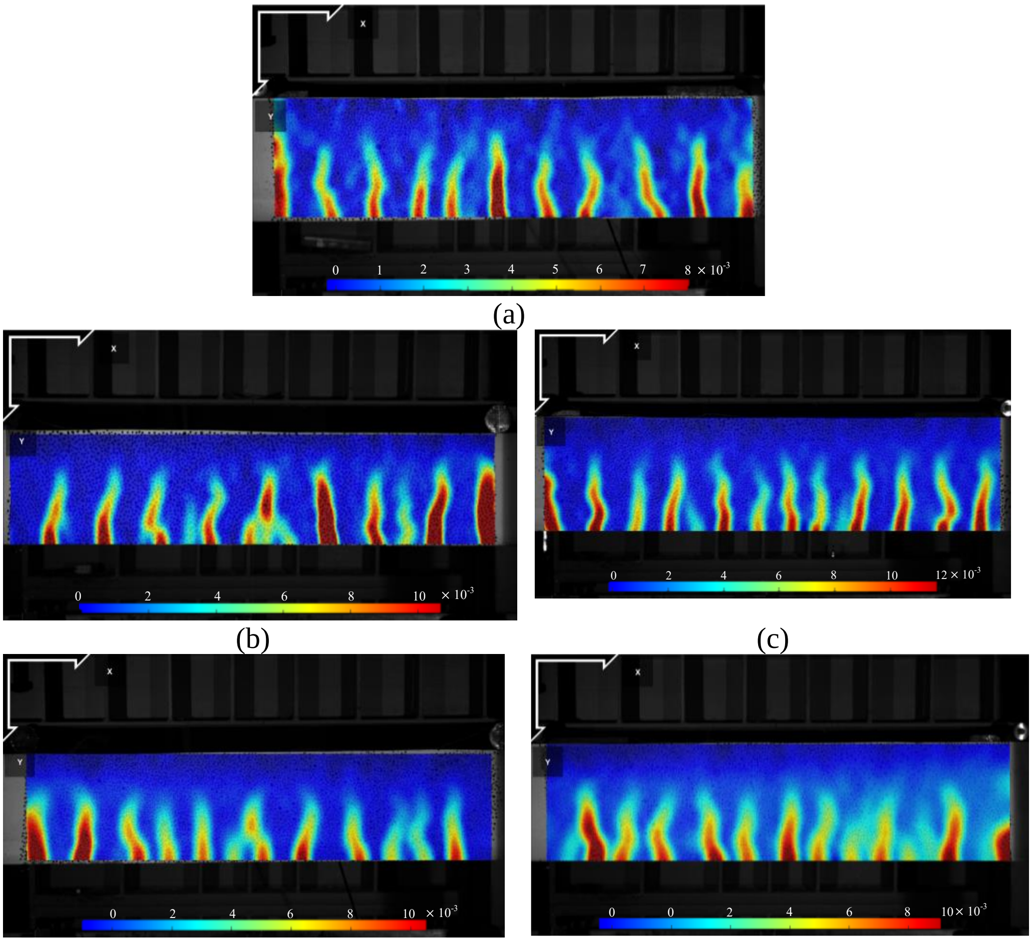

(a)

(b) (c)

d) (e)

Fig. 6. Strain contours of beams at the failure obtained from the DIC analysis: (a) B13 (b) A16 (c) B16 (d) A19 (e) B19

Since the span length of the specimens was relatively large, only the theoretical bending moment zone was considered for measurement. The total crack width was derived by integrating the strains over the length of the theoretical bending moment in the DIC analysis. These values were compared with the crack width measured using a digital crack width detector at 4 load levels: initial concrete cracking, 50% and 65% of the ultimate strength, and yielding. Table 4 shows the total crack measurement by DIC and experiment for the theoretical bending moment zone of the specimens. Table 4 shows that B-16 and B-19 specimens with greater concrete cover and reinforcement ratio had greater values of total crack width, which confirms the observations from Figure 6.

Table 4: Total crack width comparison results

Specimen	Stage	DIC	Experiment	Difference
B13	Crack	0.08 mm	0.05 mm	56.20%
	50%	0.96 mm	0.76 mm	25.66%
	65%	1.80 mm	1.42 mm	26.80%
	Yield	3.99 mm	2.91 mm	37.11%
A16	Crack	0.11 mm	0.09 mm	22.22%
	50%	1.57 mm	1.14 mm	37.63%
	65%	2.14 mm	1.75 mm	22.22%
	Yield	5.19 mm	4.83 mm	7.41%
B16	Crack	0.10 mm	0.09 mm	11.11%
	50%	2.08 mm	1.24 mm	68.00%
	65%	2.78 mm	1.9 mm	46.13%
	Yield	6.61 mm	4.52 mm	46.15%
A19	Crack	0.12 mm	0.09 mm	35.56%
	50%	1.44 mm	1.13 mm	27.86%
	65%	1.90 mm	1.77 mm	7.51%
	Yield	5.36 mm	4.72 mm	13.52%
B19	Crack	0.06 mm	0.05 mm	22.40%
	50%	2.02 mm	1.28 mm	57.48%
	65%	2.71 mm	1.93 mm	40.65%
	Yield	7.15 mm	5.48 mm	30.39%

As shown in Table 4, the total crack width measured through the DIC analysis was significantly larger than the experimentally obtained values, with differences ranging from 7.41% to 68%. The differences in the total crack width results between measurement methods can be attributed to the fact that different sides of the specimen were used for each method—DIC was applied to one side, while a crack-measuring instrument was used on the other. Additionally, the significant difference may stem from the way DIC data is processed. With the DIC method, the total crack width is calculated by integrating the strains in the theoretical bending moment zone. The DIC method records the displacement and strain across the entire surface, including both cracked and uncracked areas, thereby capturing the elastic strains of uncracked sections. In contrast, the total crack width data labeled as experimental in Table 4 were obtained through visual and manual inspection using a crack width detector. This method does not account for elastic strains, and there are also some cracks undetected due to human error.

The difference between DIC and experimental measurements is more pronounced during the first two load steps (first cracking and 50% of the ultimate load) and diminishes in the last two load steps (65% of the ultimate load and yielding load) for each specimen as shown in Table 4. This trend suggests that the elastic deformation captured by DIC plays a significant role early in the loading process, where most deformations are still elastic and cracks are just beginning to form. By the final loading, the concrete sections have already experienced cracks, reducing the impact of elastic deformation on the measurements.

IV. Conclusion

This study explores the use of the DIC method to analyze the cracking of reinforced concrete beams, considering different reinforcement ratios and concrete cover thicknesses as key parameters. The objective of this work is to verify the accuracy of the DIC method for measuring the midspan displacement and total crack width by comparing them with the results obtained using traditional measuring instruments. The findings revealed that the displacement values taken from the DIC method closely matched those measured by the LVDT, with a minimal difference of 2.33%. The total crack width values taken from the DIC were greater than those obtained by the experiment in the range of 7.41%-68%, which means that the cracks missed by the human eye and elastic deformation were captured by the DIC analysis. The results confirm the reliability of the DIC method for deformation evaluation; however, for total crack width assessment, a refinement technique is needed to exclude the elastic deformation of RC beams. Future research focuses on the development of the algorithm for displacement evaluation based on the total crack width data taken from the DIC analysis.

This paper investigates the application of the DIC method in evaluating the deformation and cracking behavior of RC beams, with different reinforcement ratios and concrete cover thicknesses. The primary objective is to assess the accuracy of the DIC method in measuring midspan displacement and total crack width, comparing these results with those obtained from traditional measuring instruments. The findings show that the displacement values measured by the DIC closely matched those obtained using the LVDT, with a difference of 2.33%. However, the total crack width measured by the DIC method was larger than that observed in the experimental measurements, with differences ranging from 7.41% to 68%. This indicates that the DIC method was able to capture cracks that were missed by the human eye and also accounted for elastic deformation.

These results validate the DIC method for deformation evaluation. However, when it comes to total crack width measurement, refinement is needed to exclude the elastic deformation. The research findings serve as a basis for future work, in which the measuring of shear cracks and development of an algorithm for deflection calculation based on total crack width data with the DIC analysis will be included.

V. Acknowledgements

This work was supported by the Technology Development Program (S3276632) funded by the Ministry of SMEs and Startups (MSS, Republic of Korea).

Conflict of interest

The authors declare no conflict of interest available for this manuscript.

References

I. Aris, A., Messa, R., Yuki, O., and Hibino, Y:'Application of Digital Image Correlation Method in RC and FRC Beams Under Bending Test'. Geomate Journal. vol. 24(101), pp:118–125,203. 10.21660/2023.101.g12275

II. Bažant, Z. P., and Cedolin, L. 'Fracture Mechanics of Reinforced Concrete'. Journal of the Engineering Mechanics Division. vol. 106(6), pp: 1287–1306,1980. 10.1061/JMCEA3.0002665

III. Bažant, Z. P., and Oh, B. H.:'Spacing of Cracks in Reinforced Concrete'.Journal of Structural Engineering. vol. 109(9), pp. 2066–2085,1983. 10.1061/(ASCE)0733-9445(1983)109:9(2066)

IV. IV. Blaber, J. A., Adair, B., and Antoniou, A.: 'Ncorr: Open-Source 2D Digital Image Correlation MATLAB Software'. Experimental Mechanics, vol. 55, pp:1105–1122,2015. 10.1007/s11340-015-0009-1

V. Ding, Y. : 'Investigations into the Relationship Between Deflection and Crack Mouth Opening Displacement of SFRC Beam'.Construction and Building Materials, vol. 25(5),pp:2432–2440,2011. 10.1016/j.conbuildmat.2010.11.055

VI. Fayyad, T. M., and Lees, J. M., 'Experimental Investigation of Crack Propagation and Crack Branching in Lightly Reinforced Concrete Beams Using Digital Image Correlation'. Engineering Fracture Mechanics, vol. 182, pp: 487–505,2017. 10.1016/j.engfracmech.2017.04.051

VII. Gali, S., and Subramaniam, K. V. L.: 'Shear Behavior of Slender and Non-Slender Steel Fiber-Reinforced Concrete Beams'. ACI Structural Journal, vol. 116, p. 149,2019.10.14359/51713307

VIII. Gupta, A. K., and Akbar, H. "Cracking in Reinforced Concrete Analysis'. Journal of Structural Engineering. vol. 110(8),pp. 1735–1746,1984. 10.1061/(ASCE)0733-9445(1984)110:8(1735)

IX. Huang, Y., He, X., Wang, Q., and Xiao, J. 'Deformation Field and Crack Analyses of Concrete Using Digital Image Correlation Method'.Frontiers of Structural and Civil Engineering. vol. 13(5),pp: 1183–1199,2019. 10.1007/s11709-019-0545-3

X. Kammers, A. D., and Daly, S., 'Small-Scale Patterning Methods for Digital Image Correlation Under Scanning Electron Microscopy'. Measurement Science and Technology.vol. 22(12), p. 125,20111. 10.1088/0957-0233/22/12/125501

XI. Lacidogna, G., Piana, G., Accornero, F., and Carpinteri, A., 'Multi-Technique Damage Monitoring of Concrete Beams: Acoustic Emission, Digital Image Correlation, Dynamic Identification'. Construction and Building Materials. vol. 242, p. 118114, 2020. 10.1016/j.conbuildmat.2020.118114

XII. Lee, H.-M., and Yoo, K.-S., 'A Study on the Metabus-Based Equipment Monitoring System'The Korean Innovation Industry Society. vol. 1(3), pp. 99–105,2023.10.60032/JIIT.2023.1.3.99

XIII. McCormick, N., and Lord, J., 'Digital Image Correlation for Structural Measurements'. Proceedings of the Institution of Civil Engineers - Civil Engineering, vol. 165(4), 2012, pp. 185–190,2012. 10.1680/cien.11.00040

XIV. Oh, B. H., and Kang, Y. J., 'New Formulas for Maximum Crack Width and Crack Spacing in Reinforced Concrete Flexural Members.'.ACI Structural Journal. vol. 84, pp: 103–112,1987. 10.14359/2787

XV. Poldon, J. J., Hoult, N. A., and Bentz. E. C., 'Distributed Sensing in Large Reinforced Concrete Shear Test'. ACI Structural Journal. vol. 116(5), 2019, pp. 235–245,2019.10.14359/51716765

XVI. Seemab, F., Schmidt, M., Bakhteer, A., Classen, M., and Chudoba, R., 'Automated Detection of Propagating Cracks in RC Beams Without Shear Reinforcement Based on DIC-Controlled Modeling of Damage Localization'.Engineering Structures. vol. 286, pp: 116–118,2023.10.1016/j.engstruct.2023.116118

XVII. Sindu, B. S., and Saptarshi, S., 'Multi-Scale Abridged Cement Composite with Enhanced Mechanical Properties'. ACI Materials Journal.vol. 117(4),2020. 10.14359/51724625

XVIII. Tambusay, A., Suryanto, B., and Suprobo, P., 'Digital Image Correlation for Cement-Based Materials and Structural Concrete Testing'. Civil Engineering Dimension. vol. 22(1), pp: 6–12,2020.10.9744/ced.22.1.6-12

XIX. Toutanji, H., and Deng, Y., 'Deflection and Crack-Width Prediction of Concrete Beams Reinforced with Glass FRP Rods'.Construction and Building Materials. vol. 17(1),pp. 69–74,2003.10.1016/S0950-0618(02)00094-6

XX. Verbruggen, S., De Sutter, S., Iliopoulos, S., Aggelis, D.G., and Tysmans, T., 'Experimental Structural Analysis of Hybrid Composite-Concrete Beams by Digital Image Correlation (DIC) and Acoustic Emission (AE)'. Journal of Nondestructive Evaluation. vol. 35(1), p. 2,2015. 10.1007/s10921-015-0321-9